Learning to Simulate and Design for Structural Engineering

Kai-Hung Chang
Autodesk Research
San Francisco, CA 94111
kai-hung.chang@autodesk.com

Chin-Yi Cheng
Autodesk Research
San Francisco, CA 94111
chin-yi.cheng@autodesk.com

Abstract

In the architecture and construction industries, structural design for large buildings has always been laborious, time-consuming, and difficult to optimize. It is an iterative process that involves two steps: analyzing the current structural design by a slow and computationally expensive simulation, and then manually revising the design based on professional experience and rules. In this work, we propose an end-to-end learning pipeline to solve the size design optimization problem, which is to design the optimal cross-sections for columns and beams, given the design objectives and building code as constraints. We pre-train a graph neural network as a surrogate model to not only replace the structural simulation for speed but also use its differentiable nature to provide gradient signals to the other graph neural network for size optimization. Our results show that the pre-trained surrogate model can predict simulation results accurately, and the trained optimization model demonstrates the capability of designing convincing cross-section designs for buildings under various scenarios.

1 Introduction

Structural design is a process to design the skeleton of a building and ensure its strength, stability, and rigidity under various load conditions. The development of powerful computers and structural simulation programs have made designing complex buildings possible. However, structural design in practice has been a laborious, slow, and iterative process for decades. Given an architectural design, structural engineers first draw the geometry of the building by determining the locations of bars (vertical columns and horizontal beams) and how they are connected. Then, details are filled in, such as cross-sections of bars. The completed structural design is highly based on professional knowledge and experience. This design is processed by a structural simulation program to compute structural properties, such as stress and story drift, using finite element analysis. Then structural engineers review the simulation results and assess if the structural design satisfies building codes, all of which are written in a dictionary-like book with hundreds of pages. Lastly, engineers need to iteratively revise the structural design and rerun the simulation until all the building codes are satisfied. The entire process can easily take weeks.

To automate structural design, we propose an end-to-end learning pipeline. Specifically, we focus on the size design optimization, which solves optimal cross-sections of bars subject to design objective and constraints. The design objective is to minimize total material cost. As for constraints, we consider 1) variety constraint in design convention, which limits the number of different cross-section types used, 2) story drift ratio limit from building codes, which prohibits story drift ratio from exceeding the limit under seismic loads. Story drift is defined as the difference between the absolute values of displacements for two consecutive stories under lateral forces, and story drift ratio is story drift divided by the height of the lower story.

Our proposed end-to-end learning pipeline leverages the differentiable nature of a pretrained Surrogate Model for structural simulation, and trains an Optimization Model for size design with the optimization objective and constraints as loss. The gradient of the loss can hence be computed with respect to the learning variables in the Optimization Model. The entire pipeline is illustrated in Figure 1. Due to the structured composition, we represent building geometries and structural designs as graphs. Accordingly, both models are graph neural networks (GNNs) to take in graph inputs.
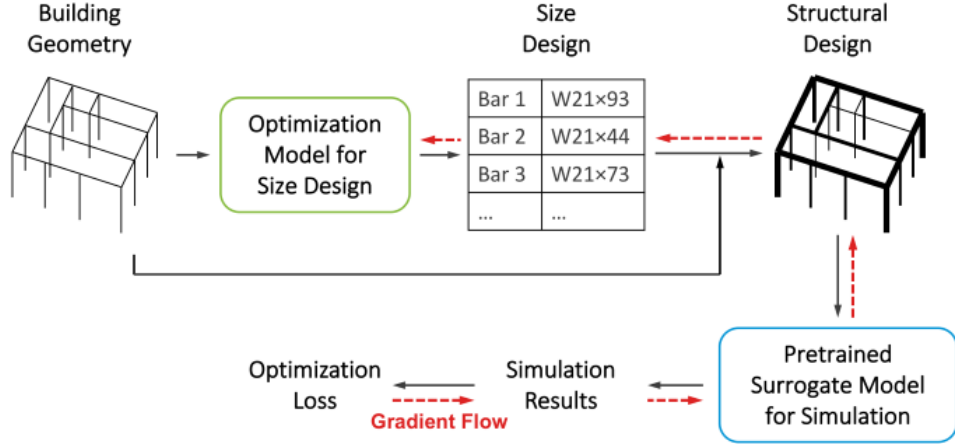
Figure 1: Our proposed end-to-end learning pipeline for solving the size design optimization problem. The differentiable Surrogate Model allows gradient of the loss function to be computed with respect to the Optimization Model.

Moreover, our GNNs are designed with structural engineering insights to achieve better performance. Results show that the Surrogate Model is able to predict structural simulation results with high accuracy and the Optimization Model is able to create convincing size designs and shows the capability of reasoning design rules that are not explicitly given.

The paper is organized as follows: Section 2 discusses related work and Section 3 describes the end-to-end learning pipeline and data generation process. Section 4 and Section 5 provide details of the Surrogate Model and the Optimization Model. All results are explained in Section 6 and Section 7 is conclusion.

2   Related Work

Most structural engineering research solveS building design problems with optimization algorithms, such as genetic algorithms [1]. These methods can be generally slow, especially when structural simulation is involved in each iteration. Papers that use machine learning approaches either use vectors to represent the specification of a structural component [2, 3, 4] or a single structure[5], or use 2D images to coarsely describe the structural geometry [6]. These research suffer from scalability and complexity and thus are far from applicable in real world scenarios.

Training neural networks for design tasks in image domain is well explored. Most task models are trained end-to-end, followed by a second differentiable model. Taking drawing task as an example, StrokeNet [7] and Canvas Drawer [8] train a neural drawer with a pretrained renderer to output stroke sequences that make up the given target image. When training the neural drawer, the approximate but differentiable renderer is frozen and passes the gradient of the unsupervised loss to the neural drawer. Similarly, [9] trains a neural program executer with a pretrained scene generator given a target 3D shape scene. Other than rendering images, the second model can be used to generate other outputs used for loss computation. [10] trains a model to output hand pose parameters which are passed to a forward kinematic layer to compute joint locations. Besides measuring supervised loss for the joint location output, they also consider a back-propagable physical constraint loss and combine them with a fixed weight. In our work, the Surrogate Model is pretrained like differentiable renderers, but to output structural simulation results. Since there's no supervision in our task, we formulate our loss with optimization objective and constraints and train the Optimization Model via on-line learning.

[11] uses a differentiable renderer in a model-based reinforcement learning (RL) framework and trains a neural drawer using the RL loss. We do not use RL due to the following two reasons. First, unlike generating hundreds of strokes to reproduce a painting, structural design is not a sequential decision making process. Moreover, since our optimization objective and constraints can be formulated as differentiable functions, there is no need to use RL loss which can lead to training instability and data inefficiency.

Different from paintings or drawings in the aforementioned work, building structures cannot be fully represented as raster images without loss of completeness. In contrast, graph is a robust representation for complex building structures, which can store not only the building geometry with graph connectivity, but also bar and building information as

node and graph features respectively. In this work, we use GNNs, which have recently shown great successes in many domains for structured data, including physics systems [12, 13, 14], chemical molecules [15, 16, 17], and traffic networks [18, 19]. Interestingly, there is an analogy between the message passing from a node to another node in GNN and the force applied to a bar (column or beam) from a neighboring bar in structural mechanics. Moreover, the numerical methods for structural simulation also have such algorithmic structure. All of the above makes GNN a promising model. Most relevant to our application, [20] trains a GNN policy to glue pairs of blocks to stabilize a tower under gravity using RL. Though the paper shows the relational inductive bias of GNN is critical in solving structured reasoning problems, their experiment setup is far from real-world engineering practice. For instance, only maximum of ten blocks is experimented. In contrast, our building structures contain up to 1500 structural components and consider lateral seismic loads besides gravitational loads.

3   Pipeline and Data Generation

3.1   End-to-End Learning Pipeline

Our goal is to train a model to solve size design optimization. The Optimization Model takes a building geometry as input and outputs cross-section types for each column and beam. The building geometry combining the proposed size design is evaluated with respect to an objective and constraints, which are computed based on structural simulation results.

Thinking about solving optimization with neural networks, one might think of model-free deep reinforcement learning (RL), which user can assign arbitrary reward and train a policy to maximize the reward via trial and error. However, one limitation is that such method requires frequent access to reward data. Unlike most RL tasks which environment is a robot simulator or a game engine, running structural simulation is slow and thus should be avoided during training.

To resolve this problem, we first pretrain a Surrogate Model that predicts structural simulation results. The results are evaluated with respect to the optimization objective and constraints. Instead of using the RL loss, which can be unstable to train, we formulate the objective and constraints as differentiable loss functions. Given the differentiable nature of the Surrogate Model, we can pass the gradient of the loss with respect to learning variables of the Optimization Model. During training, the Surrogate Model is frozen since we found the accuracy remains high throughout training and that fine-tuning the model degrades the performance even after convergence. The entire pipeline is illustrated in Figure 1.

3.2   Data Generation

To train a Surrogate Model that predicts structural simulation results, data are first generated directly from a professional structural simulation program, Autodesk Robot Structural Analysis (RSA). The structural simulation workflow and settings used in data generation process follow the industry standards and are advised by structural engineers with decades of industry experience. A fixed sampling algorithm is used to create buildings up to 10 stories on a 400 ft $\times$ 400 ft construction site. Cross-sections of bars are randomly assigned from a standardized cross-section library provided by a construction company. Multiple load cases are simulated in RSA and we save story drift ratio results to the database. Figure 2 illustrates one building example. For more details, please refer to the supplementary material.

3.3   Graph Representation

Once structural simulation is completed in RSA, the building geometry is represented and stored as a structural graph. Every bar (columns and beams) is presented as a graph node. An edge connects two nodes if the two corresponding bars are joined together. Information of bar i is stored in node feature $v_i = [p_1, p_2, B, T, L]$, where p_1 and p_2 locates the two endpoints of the bar, B indicates if the bar is a beam or a column, T is a one-hot vector representing the cross-section type, and L provides auxiliary loading condition information, including if the bar is on the roof story, if the bar is on the boundary, and the surrounding floor penal areas which are multiplied by the per-area loads when computing total load. A psuedo ground node is connected to all first-story columns and the values of its feature vector are all -1. The structural graph of a simple example structure is illustrated in Figure 3. Story level indices for each bar are also saved and used in the pooling layer of GNN to compute story output. Edge features and graph features are not used, but they can represent, for instance, structural connector properties and site information, respectively, in more complex use cases.

The average time to generate one datum is 43.91 seconds, out of which, 13.02 seconds are used to run structural simulation in RSA. 4000 structural graphs are collected, where 3200, 400, and 400 graphs are used for training, validation and testing respectively. The average number of nodes is 252.79 while the average number of edges is 1132.27. Statistics histograms are attached in the supplementary materials. Structural graphs are relatively large
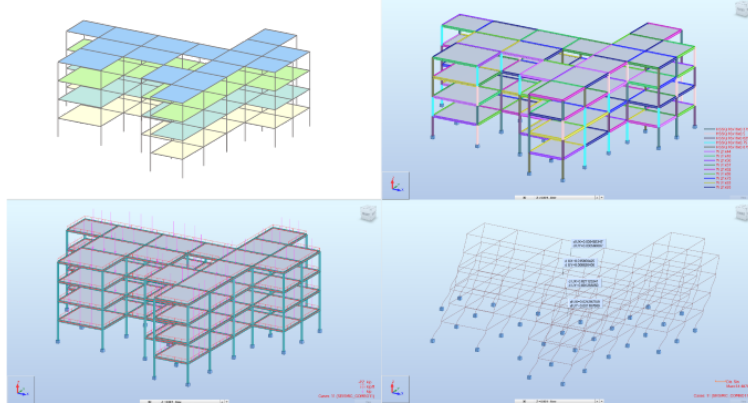
Figure 2: **Top Right**: A randomly sampled building geometry. **Top Left**: Random color-coded cross-sections. **Bottom Left**: The load conditions of the structure. **Bottom Right**: Story drift ratio results of structural simulation
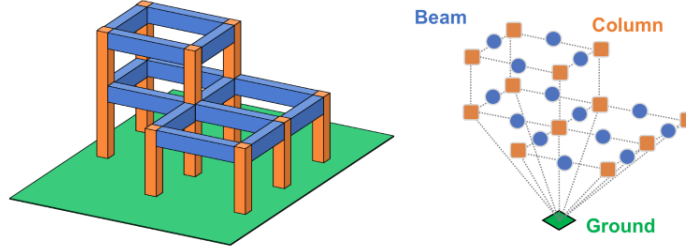

Figure 3: An example building structure and its structural graph representation.

compared to molecule graphs, but smaller than web-scale graphs such as citation graphs, social networks, and knowledge graphs. Different from web-scale graphs, which are usually passed to GNNs as partial graphs to speed up computation, structural graphs require completeness to fully represent a building structure.

4 Surrogate Model for Structural Simulation

4.1 Network Structure

Inspired by GraphNet [21], our Surrogate Model contains three steps: encoder, propagation, and decoder. First, we map each node feature into the embedding space through a single-layer perceptron (SLP) encoder.

$$v_i^0 = SLP_{encoder}(v_i) \tag{1}$$

The propagation step is then repeated multiple times to update node embeddings. Besides classic message function derived from direct neighbors, we also integrate the concept of positional-aware message from Position-Aware Graph Neural Network (PGNN) [22]. Neighbor message models the interactive force exerted from a neighboring bar while positional-aware message encodes where the node is located relative to the entire graph. Therefore, global geometric information that is useful in reasoning load computation, such as if a bar is at the boundary, can be encoded in the position-aware message. Given S amount of anchor sets $\{A_s | s = 1 \dots S\}$, the position-aware message for node i at propagation step t is computed as below:

$$mp_i^t = Mean\{SLP_{p\_message}([v_i^t, \frac{1}{d(i,j)+1}v_j^t]), j = \arg\max_l\{d(l,i)|l \in A_s\}|\forall A_s, s = 1 \dots S\} \tag{2}$$

4

, where $d(i, j)$ is the geodesic distance between node i and node j. After the aggregated neighbor messages m_i^t are computed, each node feature is updated based on the two messages and its current feature.

$$m_i^t = Mean\{SLP_{message}(v_i^t, v_j^t)|j \in Ne(i)\} \tag{3}$$

$$v_i^{t+1} = SLP_{update}(v_i^t, mp_i^t, m_i^t) \tag{4}$$

where $Ne(i)$ is the set of neighbors of node i.

After T propagation steps, the decoder is structured depending on the target tasks. If we want to predict displacements on every bar, per-node output can be computed as in Equation 5. Or, if we want to predict total mass for the entire structure, per-graph output can be computed as in Equation 6.

$$h_i = MLP_{decoder}(v_i^T) \text{ per-node output} \tag{5}$$

$$h = MLP_{decoder}(Agg(v_i^T)) \text{ per-graph output} \tag{6}$$

, where MLP is a multi-layer perceptron and Agg is an aggregation function, such as mean, max, or sum. Since our task is to generate output for all K stories, an average pooling layer is applied to all nodes on the same story:

$$o_k = AvgPool(\{v_i^T\}|i \in \text{Story } k\}) \tag{7}$$

$$o_k \leftarrow SLP_{recursive}\{[o_k, o_{k+1}]\} \text{ for } k = K - 1 \dots 1 \tag{8}$$

Here, we add a recursive structure from the top story to the bottom story as expressed in Equation 8. This is due to the fact that the lower the story, the higher the drift ratio. As a result, one fixed decoder is not capable of modeling inconsistent data distributions for buildings of different stories. Note that input normalization does not help in this case.

In the end, the story feature is passed to two MLP decoders: one predicts the story drift ratio and the other classifies if the absolute value of the ground-truth story drift ratio exceeds the building code limit lim.

$$h_k = MLP_{decoder}(o_k) \tag{9}$$

$$c_k = SigmoidMLP_{decoder}(o_k) \tag{10}$$

4.2 Loss Function

Given the two outputs in Equation 9 and 10, an L1 loss and a binary cross-entropy loss are used simultaneously.

$$\text{Loss} = \frac{1}{K}\sum_{k=1}^{K}|h_k - \hat{h}_k| - w\big(\hat{c}_k \log c_k + (1 - \hat{c}_k)\log(1 - c_k)\big) \tag{11}$$

, where $\hat{h}_k$ is the ground-truth story drift ratio , $\hat{c}_k$ is 1 if $\hat{h}_k > lim$, otherwise is 0, and w is the weight balancing the two losses.

5 Optimization Model for Size Design

5.1 Network Structure

The inputs of the Optimization Model are building geometries, which are the same as structural graphs except the node features now do not contain cross-section types. The output is the probability distribution of cross-section types for every node in the graph. Similar to the Surrogate Model, the Optimization Model also has encoder, propagation, and decoder steps. The encoder step is the same as in Equation 1. As for propagation step, the node feature is updated without the position-aware message using the below equation:

$$v_i^{t+1} = SLP_{update}(v_i^t, m_i^t) \tag{12}$$

Since size design requires consideration of the whole building, we compute a max-pooling graph embedding g to replace position-aware message, which provides only information of a bar to partial buildings.

$$g = MaxPooling(v_i^T|\forall i) \tag{13}$$

Lastly, node embeddings together with the graph embedding are fed into an MLP decoder to generate a hard Gumbel-Softmax output. The hard version returns deterministic samples as one-hot vectors to ensure consistency when training the Surrogate Model, but is differentiated as if they are the soft samples in back propagation.

5.2 Loss Function

In this section, we define the design objective and constraints.

1. Cost Objective l_c: One of the most important objectives in structural design is to minimize cost. We build a simplified material cost model by assigning unit costs for all cross-section types (regardless of the lengths of bars) as shown in Figure 6. The total cost is computed by summing the products of the unit cost and the amount of usage for each cross-section type: $l_c = \sum_{node_i} cost(type_i)$.

2. Drift Ratio Constraint l_{dr}: In the building code, the absolute value of story drift ratio is required to be less than the drift ratio limit lim. Given the predicted drift ratio of story k as h_k, the drift ratio constraint is defined as $l_{dr} = 0$ where $l_{dr} = Mean(\{ReLU(|h_k| - lim)|\forall \text{story } k\})$. In practice, to provide dense gradient signals, we use $leakyReLU$ with negative slope 0.01 instead of $ReLU$.

3. Variety Constraint l_v: This constraint comes from design conventions and limits the number of different cross-sections used. Normally, higher variety usually results in higher cost in transportation, storage, manufacturing, etc. Here we penalize usage more than 6 different cross-section types. The output of the Optimization Model can be represented as an $N \times d$ matrix, where N is the number of nodes and d is the number of cross-section types available. Summing the vectors along the N dimension, we get the bar usage histogram $H \in \mathbf{R}^d$. Instead of counting the non-zeros and taking the sum, which provides poor gradient, we sum the usage percentages of the top 6 cross-section types used. The usage percentage is computed by taking L1 norm of H: $\hat{H} = H/\sum H_i$ then summing the top 6 numbers. Ideally, the sum of top 6 numbers should be equal to 1, meaning there is zero usage of bars other than the top 6 (or less) cross-sections. Mathematically, the loss is computed as: $l_v = 1 - \sum \text{Top6}(\hat{H})$ and the constraint is $l_v = 0$

4. Entropy Constraint l_e: To avoid quick overfitting to some undesired local minimum, we need some randomness in the model. Besides adding dropouts after each propagation and at decoder, we also add entropy constraints as inspired by maximal entropy RL [23]. We compute the entropy of the size design output $\mathcal{H}$ and divide it by the maximal entropy $\mathcal{H}_{max}$. We denote the target entropy ratio as α and define the entropy constraint as $l_e = \mathcal{H}/\mathcal{H}_{max} - \alpha = 0$. In our experiments, we found that without this constraint, the model quickly converges to an undesired local minimum, which always uses one cross-section type for all columns and beams.

5.3 Adaptive Weight Optimization

When there are multiple loss functions or hard constraints, finding the optimal weights is non-trivial. Instead of having to fine-tune the weights manually, we can automate the process by optimizing the dual objective and approximating dual gradient descent [24]. This technique has been used in soft actor-critic algorithms [23] and reward constrained policy optimization [25].

A general constrained optimization problem with an objective function $f(\theta)$ and an equality constraint $g(\theta)$ can be writen as

$$\min_{\theta} f(\theta) \qquad \text{s.t. } g(\theta) = 0 \tag{14}$$

Changing the constrained optimization to the dual problem, we get the Lagrangian:

$$L(\theta, \lambda) = f(\theta) - \lambda g(\theta) \tag{15}$$

, where λ is the dual variable. Dual gradient descent alternates between optimizing the Lagrangian with respect to the primal variables to convergence, and then taking a gradient step on the dual variables. The necessity of optimizing the Lagrangian to convergence is optional under convexity.Both [23] and our work found updating one gradient step still works in practice. As a result, the primal and dual variables are iteratively updated by the following equations.

$$\theta' = \theta + \beta(\nabla_{\theta} f(\theta) - \lambda \nabla_{\theta} g(\theta)) \tag{16}$$

$$\lambda' = \lambda + \gamma g(\theta) \tag{17}$$

where β and γ are learning rates. Given an objective weight w and dual variables $w_{1 \sim 3}$, our loss function is

$$wl_c + w_1 l_{dr} + w_2 l_v + w_3 l_e. \tag{18}$$

6 Results and Discussion

6.1 Surrogate Model for Structural Simulation

The performance of our Surrogate Model is compared to that of other models, including GCN [26], GIN [27], and GAT [28]. In addition, we conduct ablation studies to show improvements in performance when using our proposed structure.
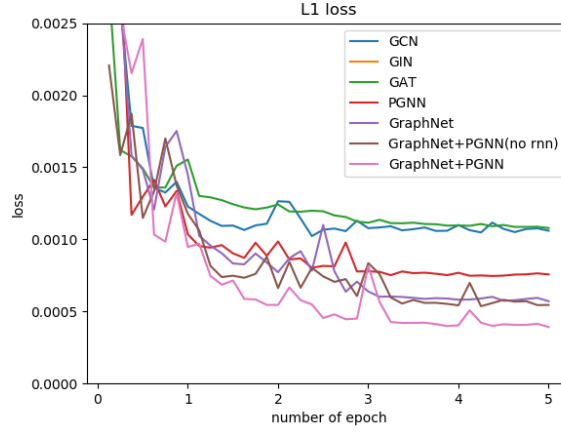
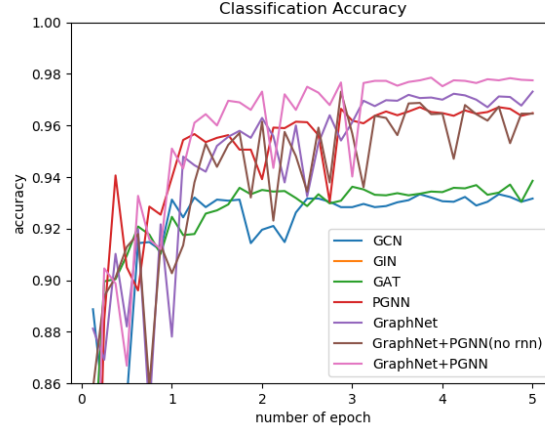Figure 4: Learning curve of L1 regression loss for story drift ratio.

Figure 5: Learning curve of classification accuracy for story drift ratio.

GraphNet+PGNN is our model which uses both neighbor and position-aware messages while GraphNet and PGNN use only neighbor and position-aware message respectively. GraphNet+PGNN(no rnn) uses both messages, but does not have the recursive structure at the decoder step. The learning curves are visualized in Figure 4 and Figure 5. Note that the curve of GIN is outside the y range of both plots.

Compared to GCN, GIN, GAT, and PGNN, GraphNet shows the best performance which indicates that GraphNet's node feature update function better models the structural simulation algorithm. The concatenated position-aware message improves the performance as expected, because it provides non-local information, which is critical when reasoning load conditions. The recursive structure at the decoder step also boosts the performance. Overall, our Surrogate Model is specifically designed with structural engineering insight to better model structural simulation and achieves the best performance.

After training, the Surrogate Model is able to predict the story drift ratio with an average L1 loss of 3.92e-4 and an average relative accuracy of 98.74% over 400 test data. The classification decoder shows 97.75% accuracy in predicting if the ground-truth is greater than the drift ratio limit. We are also interested in if the regression output has the same drift ratio limit loss as the ground-truth; i.e. if both numbers are greater or less than the drift ratio limit. The result shows that 97.69% of regression output has the same drift ratio limit loss as ground-truth. In addition, we show that the multi-task learning set-up, which trains with two outputs and two losses together, allows GNN to learn better node embeddings and achieves better performance. Last but not least, while RSA spend an average of 13,020 ms to run structural simulation, it only takes 43.92 ms for the Surrogate Model to output simulation results on a single Quadro M6000 GPU, which is almost 300 times faster.

7

Table 1: Performance of different GNN Surrogate Models

Model	L1 Loss ×1e−4	Rel. Acc.	Class. Acc.	Limit Acc.
GCN	10.06	96.75	93.17	89.12
GIN	40.30	87.08	64.79	53.63
GAT	10.08	96.83	93.85	93.58
PGNN	7.57	97.65	96.48	94.83
GraphNet	5.71	98.19	97.31	94.0
GraphNet+PGNN(no rnn)	5.45	98.28	96.46	96.52
GraphNet+PGNN	**3.92**	**98.74**	**97.75**	**97.69**
GraphNet+PGNN(L1 loss)	8.86	97.37	n/a	93.54

Class. Acc. is the accuracy of the classification prediction if the ground-truth is greater than the drift ratio limit while Limit Acc. measures the accuracy if the predicted drift ratio has the same drift ratio limit loss as the ground-truth. "n/a" means not applicable since training with l1 loss does not update the classification decoder.

6.2 Optimization Model for Size Design

The Optimization Model is trained and evaluated with two different story drift ratio limits, 0.025 and 0.015. The numbers are decided from the distribution of story drift ratio limit from collected data. The former sets a moderate constraint that there is at least one feasible solution for most buildings, while the latter sets a harsh constraint that the strongest size design might still violates it. For each limit, three different cost objective weights (w in Equation 18) -zero, low, high- are experimented. All experiments include the variety constraint and the entropy constraint. The qualitative results are listed in Table 3. The results show that both drift ratio limit and variety constraint are satisfied nicely for moderate constraint and by increasing the weight of the cost objective, structural engineers can obtain size designs of lower cost.

We visualize one size design example for all six experiments in Table 2. The histograms under each building structure plot the amount of bar usages, color-coded as in Figure 6. Based on the cross-section notations, W21×93 represents a wide-flange beam with a depth of 21 inches and has a nominal weight per foot of 93 lbf/ft. The higher the nominal weight per foot, the stronger the beam and the higher the material cost. HSSQ16×16×0.875 means square hollow structural sections with outside dimension 16 inches and wall thickness 0.875 inches. Similary, the higher the wall thickness, the stronger the column and the higher the material cost.

We show the size design figures in Table 2 to professional structural engineers and ask their feedback. Structural engineers say moderate constraint designs on the top row cannot be explained using structural design rules or knowledge and do not look like human designs. It is a surprise to them that these designs do follow the story drift ratio limit. The designs also show sophisticated decisions of cross-sections for every bar whereas structural engineers usually assign the same cross-section in groups. Interestingly, structural engineers feel more "natural" about the designs optimized under harsh constraint when seeing human design rules revealed from harsh constraint designs. These rules are reasoned by the Optimization Model and is not explicitly given during training. They are listed and explained below.

- Since the story drift ratios are measured in seismic load cases, where the lateral forces come horizontally, columns should be strengthened more than beams. This can be clearly observed from the bottom left figure that the model picks only the strongest HSSQ16×16×0.875 and HSSQ16×16×0.75 for columns but uses beams of a wide variety of strength.

- In reality, instead of considering all available cross-sections, structural engineers usually start designs with a fixed set of preferred cross-sections. This set is used for a wide variety of buildings and therefore, should cover a broad range of strength. The Optimization Model behaves similarly by mainly using W21×93, W21×73, W21×62, and W21×44 for beams in the bottom left figure.

- Given the cost model shown in Figure 6, we see that the span of cost for columns is larger than that for beams. Therefore, when cost weight is not zero and thus cost is minimized, the model uses only the weakest beam W21×44. Moreover, by making the beams weaker instead of columns, the model is able to decrease the drift ratio violation due to the structural engineering reason mentioned above.

- Since gravitational forces accumulate more at lower stories, structural engineers usually choose stronger columns for lower stories and weaker columns for higher stories to reduce cost. This is consistent to the result in the bottom right figure.

- From structural engineer's perspective, given only the objective and constraints considered in our optimization, the cross-section designs for different buildings should look similar even with irregular shape. This is consistent to our observation that the Optimization Model creates size designs with similar cross-section usage distribution for all experiments.

In other words, the design rules learned from the Optimization Model under harsh constraint is what is used to create size design by structural engineers nowadays, which can be conservative and not optimized. As a result, we show that our end-to-end learning approach for size design explores a broader design space and finds optimal solutions, which human can never create using the existing design rules.
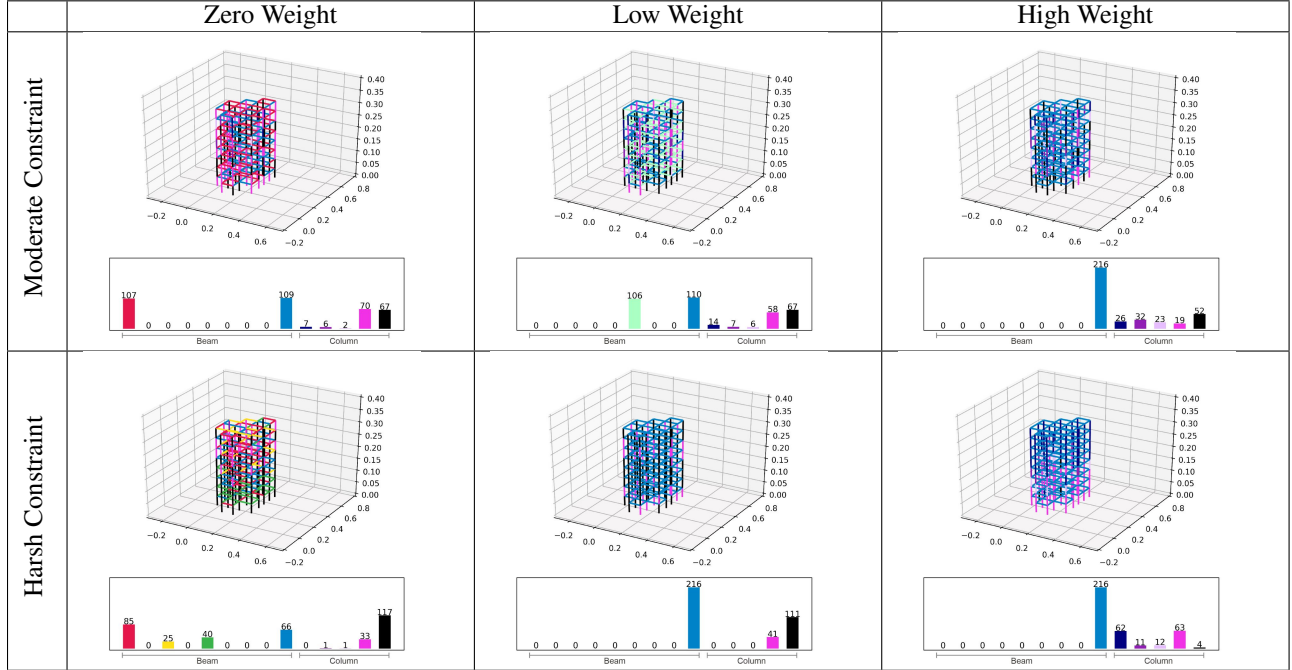
Beams: W21x93 W21x83 W21x73 W21x68 W21x62 W21x57 W21x50 W21x48 W21x44
Columns: HSSQ16x16x0.375 HSSQ16x16x0.5 HSSQ16x16x0.625 HSSQ16x16x0.75 HSSQ16x16x0.875

Table 2: Size design visualization of the Optimization Model in different experiments.
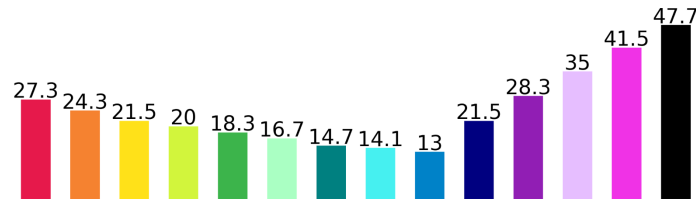

Figure 6: Cost of cross-sections, regardless of lengths of bars.

9

Table 3: Results of the optimization model for different scenarios.

Scenario	Cost Loss	Drift Ratio Loss	Variety Loss
Moderate Constraint			
Zero Weight	0.180	0.0000	0.015
Low Weight=1	0.177	0.0000	0.021
High Weight=2	0.170	0.0000	0.000
Harsh Constraint			
Zero Weight	0.206	0.0007	0.005
Low Weight=20	0.170	0.0011	0.000
High Weight=100	0.128	0.0022	0.000

7 Conclusion

In this paper, we propose an end-to-end learning pipeline to solve the size design optimization problem. To train the Optimization Model, the pipeline leverages the differentiable nature of a pretrained Surrogate Model as well as differentiable formulations for optimization objectives and constraints. Our Surrogate Model predicts structural simulation results with high accuracy thanks to the network structure specifically designed for modeling structural simulation. Taking building geometry in real-world scale as input, our Optimization Model is able to create optimal size designs for various scenarios. Last but not least, it shows the design rules reasoned under a harsh drift ratio limit matches those used by structural engineers today, which indicates human structural design is often conservative and non-optimal.

There is still much to overcome before using deep learning to fully solve structural design tasks in reality. For instance, though the randomly sampled buildings have a realistic amount of bars, real-world buildings are more complex and have other components such as joists, moment connectors, walls, and more, all of which are not considered in this work. A more complex graph representation needs to be designed to fully represent real-world buildings. Moreover, we only consider one design objective and three constraints while in real-world, the full building codes are written in a book. Though having some limitations, this research has demonstrated potentials of deep learning application in structural engineering and construction domain. We hope to arouse more research interest and see more interesting work along this direction in the future.

References

[1] T Balogh and LG Vigh. Genetic algorithm based optimization of regular steel building structures subjected to seismic effects. In *Proceedings 15th world conference on earthquake engineering*, pages 1–10, 2012.

[2] Lorenzo Greco. Machine learning and optimization techniques for steel connections. In *Proceedings of IASS Annual Symposia*, volume 2018, pages 1–8. International Association for Shell and Spatial Structures (IASS), 2018.

[3] Ahmed A Torky and Anas A Aburawwash. A deep learning approach to automated structural engineering of prestressed members. 2018.

[4] YEH Cheng, Chang-huan KOU, CHEN Li, et al. Optimal design of steel columns with axial load using artificial neural networks. *DEStech Transactions on Engineering and Technology Research*, (amme), 2017.

[5] OĞUZHAN Hasançebi and T Dumlupınar. A neural network approach for approximate force response analyses of a bridge population. *Neural Computing and Applications*, 22(3-4):755–769, 2013.

[6] Takuya Tamura, Makoto Ohsaki, and Jiro Takagi. Machine learning for combinatorial optimization of brace placement of steel frames. *Japan Architectural Review*, 1(4):419–430, 2018.

[7] Ningyuan Zheng, Yifan Jiang, and Dingjiang Huang. Strokenet: A neural painting environment. 2018.

[8] Kevin Frans and Chin-Yi Cheng. Unsupervised image to sequence translation with canvas-drawer networks. *arXiv preprint arXiv:1809.08340*, 2018.

[9] Yonglong Tian, Andrew Luo, Xingyuan Sun, Kevin Ellis, William T Freeman, Joshua B Tenenbaum, and Jiajun Wu. Learning to infer and execute 3d shape programs. *arXiv preprint arXiv:1901.02875*, 2019.

[10] Xingyi Zhou, Qingfu Wan, Wei Zhang, Xiangyang Xue, and Yichen Wei. Model-based deep hand pose estimation. *arXiv preprint arXiv:1606.06854*, 2016.

[11] Zhewei Huang, Wen Heng, and Shuchang Zhou. Learning to paint with model-based deep reinforcement learning. In *Proceedings of the IEEE International Conference on Computer Vision*, pages 8709–8718, 2019.

[12] Thomas Kipf, Ethan Fetaya, Kuan-Chieh Wang, Max Welling, and Richard Zemel. Neural relational inference for interacting systems. *arXiv preprint arXiv:1802.04687*, 2018.

[13] Alvaro Sanchez-Gonzalez, Nicolas Heess, Jost Tobias Springenberg, Josh Merel, Martin Riedmiller, Raia Hadsell, and Peter Battaglia. Graph networks as learnable physics engines for inference and control. *arXiv preprint arXiv:1806.01242*, 2018.

[14] Nicholas Watters, Daniel Zoran, Theophane Weber, Peter Battaglia, Razvan Pascanu, and Andrea Tacchetti. Visual interaction networks: Learning a physics simulator from video. In *Advances in neural information processing systems*, pages 4539–4547, 2017.

[15] Alex Fout, Jonathon Byrd, Basir Shariat, and Asa Ben-Hur. Protein interface prediction using graph convolutional networks. In *Advances in neural information processing systems*, pages 6530–6539, 2017.

[16] Wengong Jin, Kevin Yang, Regina Barzilay, and Tommi Jaakkola. Learning multimodal graph-to-graph translation for molecular optimization. *arXiv preprint arXiv:1812.01070*, 2018.

[17] Kien Do, Truyen Tran, and Svetha Venkatesh. Graph transformation policy network for chemical reaction prediction. In *Proceedings of the 25th ACM SIGKDD International Conference on Knowledge Discovery & Data Mining*, pages 750–760, 2019.

[18] Shengnan Guo, Youfang Lin, Ning Feng, Chao Song, and Huaiyu Wan. Attention based spatial-temporal graph convolutional networks for traffic flow forecasting. In *Proceedings of the AAAI Conference on Artificial Intelligence*, volume 33, pages 922–929, 2019.

[19] Zhiyong Cui, Kristian Henrickson, Ruimin Ke, and Yinhai Wang. Traffic graph convolutional recurrent neural network: A deep learning framework for network-scale traffic learning and forecasting. *IEEE Transactions on Intelligent Transportation Systems*, 2019.

[20] Jessica B Hamrick, Kelsey R Allen, Victor Bapst, Tina Zhu, Kevin R McKee, Joshua B Tenenbaum, and Peter W Battaglia. Relational inductive bias for physical construction in humans and machines. *arXiv preprint arXiv:1806.01203*, 2018.

[21] Peter W Battaglia, Jessica B Hamrick, Victor Bapst, Alvaro Sanchez-Gonzalez, Vinicius Zambaldi, Mateusz Malinowski, Andrea Tacchetti, David Raposo, Adam Santoro, Ryan Faulkner, et al. Relational inductive biases, deep learning, and graph networks. *arXiv preprint arXiv:1806.01261*, 2018.

[22] Jiaxuan You, Rex Ying, and Jure Leskovec. Position-aware graph neural networks. *arXiv preprint arXiv:1906.04817*, 2019.

[23] Tuomas Haarnoja, Aurick Zhou, Kristian Hartikainen, George Tucker, Sehoon Ha, Jie Tan, Vikash Kumar, Henry Zhu, Abhishek Gupta, Pieter Abbeel, et al. Soft actor-critic algorithms and applications. *arXiv preprint arXiv:1812.05905*, 2018.

[24] Stephen Boyd and Lieven Vandenberghe. *Convex optimization*. Cambridge university press, 2004.

[25] Joshua Achiam, David Held, Aviv Tamar, and Pieter Abbeel. Constrained policy optimization. In *Proceedings of the 34th International Conference on Machine Learning-Volume 70*, pages 22–31. JMLR. org, 2017.

[26] Thomas N Kipf and Max Welling. Semi-supervised classification with graph convolutional networks. *arXiv preprint arXiv:1609.02907*, 2016.

[27] Keyulu Xu, Weihua Hu, Jure Leskovec, and Stefanie Jegelka. How powerful are graph neural networks? *arXiv preprint arXiv:1810.00826*, 2018.

[28] Petar Veličković, Guillem Cucurull, Arantxa Casanova, Adriana Romero, Pietro Lio, and Yoshua Bengio. Graph attention networks. *arXiv preprint arXiv:1710.10903*, 2017.

A   Data Collection

This section describes the data collection process in detail. All unit abbreviations are listed in Table 4. We use the beam spans, materials, cross-sections, and load cases used by a modular construction company which developed a system of standardized components that makes designing 2-to-12-story buildings faster.

Table 4: Unit Abbreviation

Abbreviation	Full Unit
ft	Foot
pcf	Pound per cubic foot
psf	Pound per square foot

A.1   Geometry Definition

Building geometries are created by a fixed sampling algorithm due to the deficiency of real-world data. The two sides of the rectangular building bases are sampled between 60 ft to 400 ft, on which a structural grid is created given the set of beam spans ranging from 28 ft to 40 ft. A connected layout is sampled on the grid using depth-first-search algorithm which expands to neighboring grid cells with 0.5 probability. The same layout is vertically stacked up multiple stories to form a voxel-like building geometry. Each voxel contains four columns on four vertical sides and four beams which form a rectangle frame on the top to support the floor panel. Buildings collected for training the Surrogate Model contain $1 \sim 10$ stories while buildings sampled for training the Optimization Model contain $5 \sim 10$ stories. The story height is fixed at 16 ft.

A.2   Creating Structural Simulation Model in RSA

Given the geometry of the building structure, we can create the structural simulation model in Autodesk Robot Structural Analysis (RSA) program, a professional software used by structural engineers in industries. All bars (columns and beams) are placed based on the building geometry and story indices are allocated accordingly. All the columns on the first floor are fixed to the ground. Materials for columns and beams are Steel A500-46 and Steel A992-50 respectively. For each bar, the cross-section is randomly assigned from the cross-section library in Table 5. 150 pcf Concrete floor panels are modeled as slabs on trapezoid plates with other parameters given in Table 6. The definition of the symbols can be found in this link. Instead of modelling the three joists (small parallel beams across beams to support floor panels) in graph representation, each surface load is evenly distributed to six locations on the longer edges as concentrated loads.

Table 5: Cross-Section Library

Column	Beam
HSSQ 16x16x0.375	W 21 x 44
HSSQ 16x16x0.5	W 21 x 48
HSSQ 16x16x0.625	W 21 x 50
HSSQ 16x16x0.75	W 21 x 57
HSSQ 16x16x0.875	W 21 x 62
	W 21 x 68
	W 21 x 73
	W 21 x 83
	W 21 x 93

Table 6: Floor Panel Specification

Parameter Name	Value
h	6.3 in
h1	2.56 in
a	7.4 in
a1	1.73 in
a2	4.96 in
Th	7.46 in
Th 1	8.86 in
Th 2	6.3 in
Joist Direction	Parallel to the shorter edge
Material	Concrete
Material Resistance	3.5 ksi
Material Unit Weight	0.15 kip/ft3
Diaphragm	Rigid
Load Transfer	Simplified one way
Finite Element	None

A.3 Load Cases Setup

IBC 2000 is the building code used for structural simulation. Below lists all the load cases:

1. Self Weight: This is the self-weight load acting in the gravitational direction for all structure elements. The coefficient is set to 1.1.

2. Super-Imposed Dead Load: Super-imposed dead load accounts for the static weight of the non-structure elements. Here we add 24 psf surface load to all floor panels except the roof.

3. Live Load: Live load refers to the load that may change over time, such as people walking around. We consider 100 psf surface load on all floor panels except the roof.

4. Roof Live Load: Roof live load is set as 20 psf surface load, different from the live load on other stories.

5. Roof Dead Load: We assign 15 psf surface load for non-structure elements on roof panels.

6. Cladding Load: 20 psf $\times$ H(story height=16 ft) $+$ 90 $^{lb}/_{ft}$ $=$ 410 $^{lb}/_{ft}$ line load is added to all boundary beams on each story for weights of cladding walls.

7. Modal Analysis: Modal analysis determines eigenvalues (eigenpulsations, eigenfrequencies or eigenperiods), precision, eigenvectors, participation coefficients and participation masses for the problem of structure eigenvibrations. The number of modes is set to 30.

8. Seismic X: Seismic loads are automatically computed by RSA given the building code. We consider seismic loads in two directions: X and Y. Settings of seismic loads are listed in Table 7. Seismic X refers to the seismic load in direction X.

9. Seismic Y: This is the seismic loads in direction Y.

10. Static Load Combination: Load combination linearly combines multiple load cases. Static load combination is defined as $1.2D + 1.6L + 0.5L_r$, where D is the sum of dead loads (1+2+5+6), L is the live load (3),and L_r is the roof live loads (4).

11. Seismic Load Combination X: Complete quadratic combination (CQC) is used for seismic load combination. This is defined as $0.9D + 1.0E_x$, where E_x is the Seismic X load (8).

12. Seismic Load Combination Y: This is defined as $0.9D + 1.0E_y$, where E_y is the Seismic Y load (9).

A.4 Saved Results

After running the structural simulation, we save the story drift ratios in direction X and Y for Seismic Load Combination X and Y load cases respectively, since the values in the other directions are relatively small compared to the story drift ratio limit. Each story drift ratio is normalized to $[-1, 1]$.

Table 7: Seismic Parameters

Parameter Name	Value
Site Class	D
S_1 (Acceleration parameter for 1-second period)	0.6
S_s (Acceleration parameter for short periods.)	1.8
Ie (Importance factor)	0.0
Load to mass conversion for dead load	1.0
Load to mass conversion for live load	0.1
Load to mass conversion for roof live load	0.25

A.5 Statistics

Figure 7 shows statistics of the collected 4000 building structural graphs. Figure 8 plots the histogram of times to generate one datum and calculation times spent on solving each structural simulation.

(a) Number of nodes distribution.

(b) Number of edges distribution.
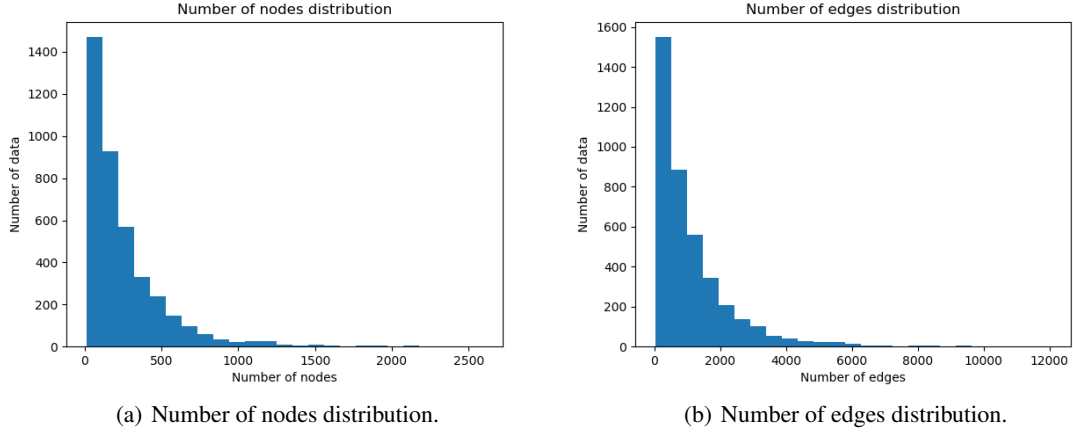
Figure 7: Statistics of 4000 collected structural graphs.

(a) Data collection time distribution.

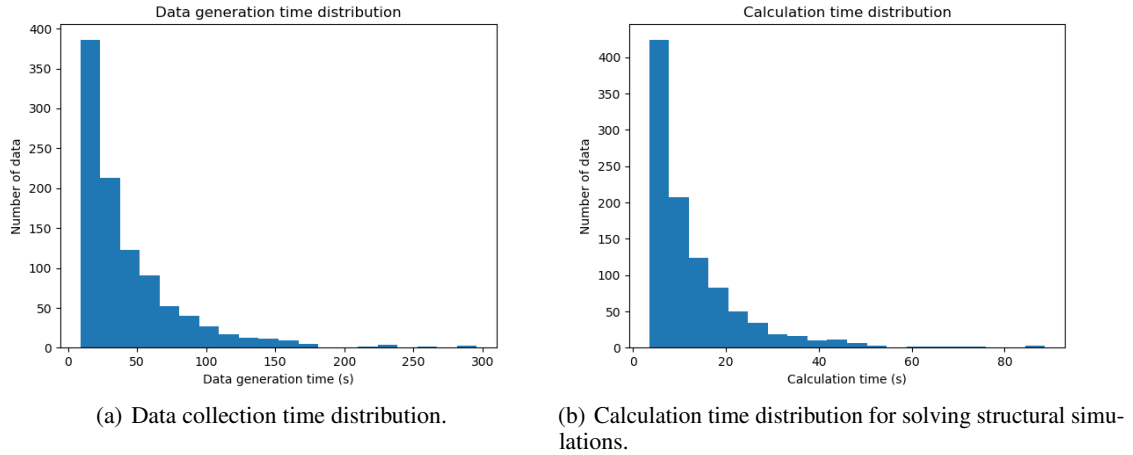(b) Calculation time distribution for solving structural simulations.

Figure 8: Statistics of 4000 collected structural graphs.

Algorithm 1 Surrogate Model for Structural Simulation

    Encoder($[19, 512]$)
    for $i = 1$ **to** 5 **do**
        p_Message($[1024, 512], ReLU$)
        Message($[1024, 512]$)
        Update($[1536, 512]$)
        Dropout
    end for
    AvgPooling
    for $i = 1$ **to** Max Story K **do**
        recursive($[1024, 512]$)
    end for
    decoder($[512, 64, 16, 2], ReLU$)
    sigmoid_decoder($[512, 64, 16, 2], Sigmoid$)

Algorithm 2 Optimization Model for Size Design

    Encoder($[10, 512]$)
    for $i = 1$ **to** 4 **do**
        Message($[1024, 512]$)
        Update($[1024, 512]$)
        ReLU
        Dropout
    end for
    MaxPooling
    decoder($[1024, 64, 32, 10], ReLU$)
    Gumbel-SoftMax

B   Hyperparameters and Training Process

B.1   Surrogate Model for Structural Simulation

The dimension of the input node features is 19, hidden dimension remains 512 before the output decoder, and the output dimension is 2. The number of anchor sets used in position-aware message computation is set to 512. Algorithm 1 shows the network structure of the Surrogate Model. The training converges after 5 epochs with batch size 1 and learning rate 1e-4. The L1 loss and the binary cross-entropy loss are weighted equally with $w = 1$.

B.2   Optimization Model for Size Design

The dimension of the input node feature is 10, hidden dimension is 512, and the output dimension is 9. Algorithm 2 shows the network structure of the Optimization Model. The model is trained with 50,000 randomly-sampled data with batch size 5 and learning rate 1e-4. A fixed 500 data set is used for evaluation. The initial weights and their learning rates for adaptive weight optimization are listed in Table 8. The drop out probability is 0.5 and linearly decays to zero at the end of training.

C   User Study

Since it is interesting to compare human designs to designs created by our models, we invite a structural engineer to work on a design in our user study. The design is a 4-story building and we give human 5 chances to propose a size design, run the structural simulation, read the simulation results, and modify the size design accordingly. We also run our Optimization models to create size designs but only once for each model. All result designs are evaluated in terms of cost, story drift ratio limit constraint(< 0.025), and variety constraint(< 6). The evaluation results are organized in Table 9. The yellow-colored row highlights the most low-cost designs that satisfy all constraints for both the structural engineer and the Optimization Model. The red cell indicates that the story drift ratio exceeds the limit. The designs are visualized in Table 10.

Table 9 shows that the performance of the first five human designs cannot surpass that of designs created by our models. Starting with a conservative design, the structural engineer gets a reference baseline and then tries to improve the

15

Table 8: Adaptive Weight Optimization Parameters

Loss	Initial Weight	Learning Rate
Cost Loss	$w = 1, 2, 20, 100$	n/a
Drift Ratio Loss	$w_1 = 1e3$	$\gamma_1 = 1e\text{-}1$
Variety Loss	$w_2 = 1.0$	$\gamma_2 = 5e\text{-}4$
Entropy Loss	$w_3 = 1.0$	$\gamma_3 = 1e\text{-}3$

performance iteratively. In the third iteration, the cost of the design decreases to 9710.8, but when the structural engineer tries to further decrease the cost in the fourth and fifth iteration, both designs violate the story drift ratio limit constraint. All Optimization Models satisfy the story drift ratio limit with zero or low variety constraint violation. Except for Zero Weight under Harsh Constraint, all other Optimization Models have lower costs than the most optimal human design.

As a result, structural engineer fails to create more optimal design than our Optimization Models within five iterations. Potentially, human might still be able to create more optimal designs given more iterations, but using our models can provide a better starting point and expedite the iterative process. Structural engineers can later fine-tune the size design created by the Optimization Model. Moreover, the 4-story building example is relatively simple. As the building design gets more complex(10 stories with more than 500 bars for example), the performance of structural engineers can drop. In contrast, since our Optimization Model trains on $5 \sim 10$ story buildings, it is scalable to more complex building designs.

Table 9: User Study Results.

Experiment	Total Cost	Beam Usage	Column Usage	Drift Ratios in Seismic X (Limit = 0.025)				Drift Ratios in Seismic Y (Limit = 0.025)			
				Story 1	Story 2	Story 3	Story 4	Story 1	Story 2	Story 3	Story 4
Human											
Iteration 1	10662.8	188, 0, 0, 0, 0, 0, 0, 0, 0, 0	0, 0, 0, 62, 62	0.0209	0.0174	0.015	0.0094	0.0207	0.0173	0.0149	0.0093
Iteration 2	11047.2	188, 0, 0, 0, 0, 0, 0, 0, 0, 0	0, 0, 0, 0, 124	0.0213	0.0178	0.0135	0.0084	0.0211	0.0177	0.0134	0.0083
Iteration 3	9710.8	0, 0, 0, 0, 0, 0, 0, 0, 0, 188	0, 0, 0, 62, 62	0.0208	0.0173	0.0149	0.0093	0.0206	0.0172	0.0148	0.0093
Iteration 4	6462.0	0, 0, 0, 0, 0, 0, 0, 0, 0, 188	124, 0, 0, 0, 0	0.0305	0.0253	0.0192	0.0119	0.0302	0.0251	0.0191	0.0119
Iteration 5	9604.3	47, 0, 47, 0, 47, 0, 0, 47	124, 0, 0, 0, 0	0.0306	0.0253	0.0193	0.0119	0.0303	0.0251	0.0191	0.0119
Moderate Constraint											
Zero Weight	9158.3	87, 0, 0, 0, 0, 0, 0, 101	1, 3, 2, 54, 64	0.0228	0.0184	0.0152	0.0111	0.0223	0.0178	0.0148	0.0109
Low Weight = 1	8151.5	0, 0, 0, 0, 83, 0, 0, 105	6, 4, 2, 41, 71	0.0210	0.0187	0.0143	0.0090	0.0208	0.0184	0.0142	0.0091
High Weight = 2	7143.5	0, 0, 0, 0, 0, 0, 0, 188	18, 15, 21, 30, 40	0.0204	0.0206	0.0153	0.0105	0.0203	0.0204	0.0152	0.0105
Harsh Constraint											
Zero Weight	9840.6	79, 0, 9, 0, 52, 0, 0, 0, 0, 48	0, 0, 0, 0, 124	0.0213	0.0177	0.0135	0.0082	0.0211	0.0175	0.0133	0.0083
Low Weight = 20	8110.8	0, 0, 0, 0, 0, 0, 0, 188	0, 0, 0, 40, 84	0.0215	0.0183	0.0136	0.0085	0.0212	0.0181	0.0135	0.0084
High Weight = 100	7078.3	0, 0, 0, 0, 0, 0, 0, 188	19, 7, 7, 90, 1	0.0228	0.0184	0.0152	0.0111	0.0223	0.0178	0.0148	0.0109
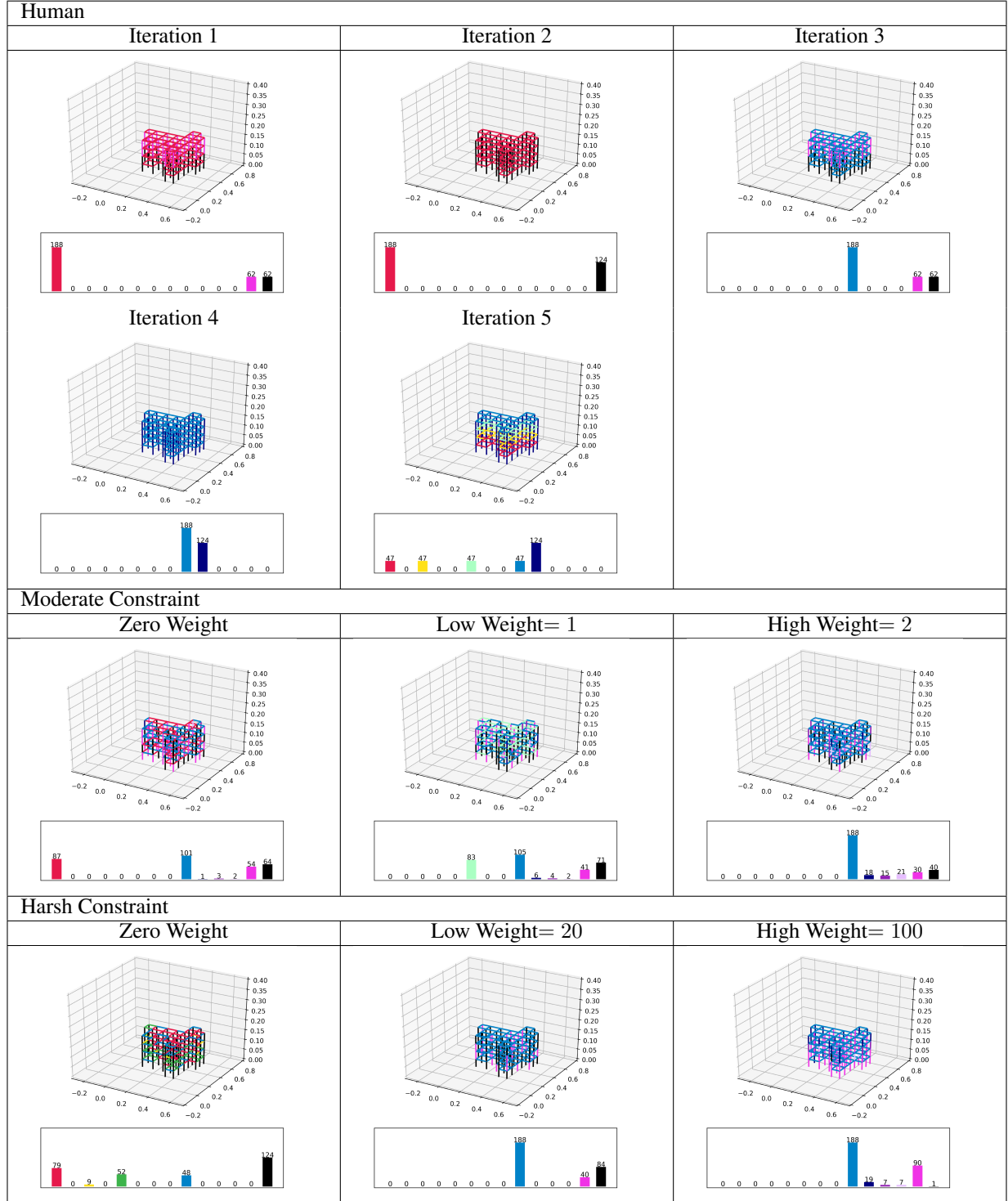
17

Beams: W21x93 W21x83 W21x73 W21x68 W21x62 W21x57 W21x50 W21x48 W21x44
Columns: HSSQ16x16x0.375 HSSQ16x16x0.5 HSSQ16x16x0.625 HSSQ16x16x0.75 HSSQ16x16x0.875

Table 10: User study visualization.